# Supplementary Appendix

**A Novel LncRNA SNHG3 Promotes Osteoblast Differentiation through Upregulating**

**BMP2 in Aortic Valve Calcification**

**Brief title: The role of SNHG3 in calcific aortic valve disease.**

Long Chen, MD [a#], Hanning Liu, MD, PhD [a#], Cheng Sun, MD, PhD [a], Jianqiu Pei, PhD [a],

Jun Li, MD [a], Yue Li, PhD [a], Ke Wei, MD, PhD [a], Xiaoyi Wang, MD [a], Peng Wang, MD [a],

Fangzhou Li, MD [a], Shujie Gai, MD, PhD [a], Yan Zhao, MD [a], and Zhe Zheng, MD, PhD [a*]

**Author's affiliations:**

[a] Department of Cardiovascular Surgery, State Key Laboratory of Cardiovascular Disease,

National Center for Cardiovascular Disease, China & Fuwai Hospital, Chinese Academy of

Medical Sciences & Peking Union Medical College, No. 167 Beilishi Road, Xicheng District,

Beijing 100037, People's Republic of China.

* Address for correspondence: Zhe Zheng, email: zhengzhe@fuwai.com (Z.Z.), Tel: +86-8839-

6051, Fax: +86-8839-6051.

[#] These authors contributed equally to this work and should be considered as co-first authors.

**Detailed Materials and Methods**

**Clinical sample**

This study was performed with the approval of the institutional Ethics Committees of the Fuwai hospital, Chinese Academy of Medical Sciences and complied with the Declaration of Helsinki (No.2012-404). All the patients signed the written informed consent before participating in the study. Human calcific aortic valve leaflefts were obtained from patients with CAVD during aortic valve replacement. Control non-mineralized aortic valves were collected from the explanted hearts of patients who underwent heart transplantation procedures. The clinical characteristic patients for lncRNA Sequencing are shown in **Supplementary Table 1** and for RT-qPCR analysis are shown in **Supplementary Table 2**. The calcification staining for human aortic valve tissues are shown in **Supplementary Figure 1**.

**Primary human valvular interstitial cells isolation and culture**

HVICs were isolated from noncalcified aortic valves obtained from patients undergoing heart transplantation. The clinical characteristics of patients are shown in **Supplementary Table 3**. Primary hVICs were isolated, and purity of the cell preparation was confirmed as described previously (1). Briefly, aortic valve leaflets were digested in 1 mg/ml collagenase (type I) at 37°C for 30 minutes, vortexed to remove endothelial cells, and further digested with a fresh solution of 4.5 mg/ml collagenase at 37°C for 1 hour. After repeated aspirations to break up the tissue fragments, the cell suspension was gently spun at 1000 rpm for 10 min to precipitate cells. Isolated cells were resuspended, seeded, and then cultured in Dulbecco′s modified Eagle′s

41    medium (Gibco, Invitrogen Corporation, Carlsbad, CA, USA) containing 100 μg/mL

42    streptomycin (Gibco), 10% fetal bovine serum, and 100 U/mL penicillin (Gibco) at 37°C

43    supplied with 5% $CO_2$ atmosphere. All experiments involving hVICs were performed on cells

44    from independent patients. Cell between passages 3 to 7 were chosen for further experiments

45    and incubated with an osteogenic induction medium to stimulate osteogenic differentiation as

46    previously described (2), which was consisted of DMEM + 5% FBS, $10^{-7}$ M insulin, 50 μg/ml

47    ascorbic acid and $NaH_2PO_4$ at 2 mM.

48    **Real-time polymerase chain reaction**

49    RNA was extracted from aortic valve tissues and cells during in vitro experiments. Total RNA

50    was isolated with Trizol reagent (Invitrogen Corporation, CA), and then was reverse transcribed

51    into cDNA using PrimeScript RT Master Mix (RR036A, Takara, JA). Real-time quantitative

52    PCR was performed with TB Green Premix Ex Taq II (RR820A, Takara, JA) according to the

53    manufacturer's recommendations. The reactions were carried out in QuantStudio™ 5 System

54    (Applied Biosystems Inc, USA) with gene-specific primers. The primers were designed on the

55    website of Primer Bank (https://pga.mgh.harvard.edu/primerbank/) and PrimerBlast

56    (https://www.ncbi.nlm.nih.gov/tools/primer-blast/index.cgi?LINK_LOC=BlastHome). All the

57    primer sequences used in this research are listed in **Supplementary Table 5**.

58    **Subcellular RNA fractionation of hVICs**

59    Nuclear and cytoplasmic RNA was purified according to manufacturer's recommendation of

60    the Nuclear and Cytoplasmic RNA Purification Kit (21000, Norgen Biotek, Canada). Then,

61　nuclear RNA fractionation was centrifuged for 2 min at 16,400 x g at 4°C to separate the nuclear

62　soluble fraction in the supernatant from the chromatin-associated fraction in the nuclear

63　remaining pellet and then the expression of SNHG3 in different subcellular fractionations was

64　analyzed by RT-qPCR. The expression of GAPDH was used as a cytoplasmic control, and U6

65　and lncRNA H19 was used as a nuclear control.

66　**Western blotting**

67　Protein was extracted from cells using RIPA lysis buffer containing protease and phosphatase

68　inhibitors (Thermo Scientific, USA), separated by sodium dodecyl sulfate-polyacrylamide gel

69　electrophoresis (SDS-PAGE) gel, transferred to polyvinylidene difluoride membranes.

70　Membranes were incubated with primary antibodies overnight at 4°C, followed by anti-mouse

71　or rabbit horseradish peroxidase (HRP)-conjugated secondary antibodies (7076/7074, CST,

72　dilution, 1:1000). Afterwards, the protein-antibody complex was visualized by enhanced

73　chemiluminescence assay (34095, Pierce). Primary antibodies against Osteopontin (ab166709,

74　abcam, dilution 1:1000), Osteocalcin (ab133612, abcam, dilution 1:1000), RUNX2 (D1L7F,

75　CST, dilution 1:1500), BMP2 (ab14933, abcam,1:2000), pSmad1/5 (D5B10, CST, dilution

76　1:1000), Smad1 (D59D7, CST, dilution 1:1000), EZH2(ab191250, abcam, 1;1000), H3(ab1791,

77　abcam, dilution 1:1000), H3K27me3 (ab6002, abcam, dilution 1:1000), GAPDH (14C10, CST,

78　dilution 1:2000) were used.

79 **RNA in situ hybridization**

80 RNA-FISH Cy3-labelled SNHG3 probes were synthesized from RiboBio (Guangzhou, China).

81 RNA-FISH assays were conducted using fluorescent in situ hybridization kit (RiboBio,

82 Guangzhou, China) according to the manufacturer's recommendation. Briefly, cells plated in

83 confocal dishes ($2\times10^4$/dishes) were fixed by 4% formaldehyde in PBS for 10 min at room

84 temperature, permeabilized with 1% Triton X-100 for another 15min, and then rinsed once in

85 $2 \times$ SSC. After that, hybridization was carried out at 37℃ for 10-15 hours using Cy3-labeled

86 SNHG3. Finally, the cells were stained with 4′-6-diamidino-2-phenylindole (DAPI) to show

87 the nuclear. Images were taken with a fluorescence microscope (Lecia, Wentzler, Germany)

88 and merged using Image Pro-Plus software (Media Cybernetics, Bethesda, MD).

89 **Detection of alkaline phosphatase activity (ALP)**

90 Alkaline phosphatase activity (ALP) in the cell lysates was assayed using a colorimetric assay

91 kit (Biovison, K412-500, SF, USA) by measuring the p-nitrophenol release in absorbance at

92 405 nm. Results are presented as relative ALP activity normalized to that of the control cells.

93 **Determination of calcium concentrations**

94 Calcium content in cell cultures was determined by the Arsenazo III method (Synermed,

95 Monterey Park, CA, USA), which depends on the specific reaction of Arsenazo III with calcium

96 to produce a blue complex. Results are measured at 650 nm on a spectrophotometer (Infinite

97 M200 Pro, Tecan, Männedorf, Switzerland). This reaction is specific for calcium. Magnesium

98 is prevented from forming a complex with the reactive.

99      **Alizarin Red S staining of cultured cells**

100     Cells were stained with 2% Alizarin Red solution. Alizarin Red solution was prepared by

101     dissolving 2 g Alizarin Red (Sigma Aldrich, USA) in 100 mL distilled water and mixing well,

102     and the pH was adjusted to 4.2 with 1 mM NaOH. The stained cells were then incubated for 30

103     min in 10% acetic acid to quantify the calcium deposition, and the absorbance was read at 405

104     nm with a spectrophotometer (Infinite M200 Pro, Tecan, Männedorf, Switzerland).

105     **High-throughput lncRNA sequencing and data analysis**

106     Gene expression was evaluated in human aortic valve tissues explanted from patient of aortic

107     valve replacement or heart transplantation. Total RNA from different experimental groups were

108     extracted. First, ribosomal RNA (rRNA) was removed by Ribo-Zero ™ rRNA Removal Kit

109     (Epicentre). Sequencing libraries were prepared from the rRNA-depleted RNA by NEBNext®

110     Ultra ™ Directional RNA library Prep Kit for Illumina® (New England Biolabs) following

111     manufacturer's recommendations, and then sequenced on the Illumine HiSeq 2500 platform by

112     Novogene (China) and 100 bp paired end reads were generated. Clean data (clean reads) were

113     obtained through in-house Perl scripts by removing reads containing adapter, reads containing

114     ploy N and low-quality reads from raw data, and aligned to the *homo sapiens* GRCh38.p12

115     genome using TopHat2 v2.0.9 (3). The mapped reads of each sample were assembled by

116     StringTie (v1.3.1) (4). Transcripts predicted with coding potential by either/all of the four tools

117     [Coding-Non-Coding-Index (CNCI) (v2) (5), CPC (0.9-r2) (6), Pfam Scan (v1.3) (7) and

118     PhyloCSF (v20121028) (8)] were filtered out, and those without coding potential were

119    candidate set of lncRNAs. Quantile normalization and subsequent data processing was

120    performed using the R software limma package (9). Normalized Intensity of each group

121    (averaged normalized intensities of replicate samples, log2 transformed) were analyzed by

122    paired t-test (P value cut off: 0.05). Volcano plot filtering was performed to show differentially

123    expressed lncRNAs with statistical significance between two groups. The distinguishable

124    lncRNAs expression pattern among samples were identified through hierarchical clustering.

125    The sequncing data of human aortic valves have been deposited in the Gene Expression

126    Omnibus (GEO) database under accession number GSE199718. Deregulated mRNAs due to

127    the absence or overexpression of SNHG3 were analyzed by Gene Set Enrichment Analysis

128    GSEA with gesaplot2 R package (10). Gene set enrichment analysis (GSEA) was applied using

129    annotations from hallmark gene sets to reduce noise and redundancy (11).

130    **Cell transfection**

131    For transfection of ASOs, cells were transfected with Lipofectamine iMax (Invitrogen, MA,

132    USA) following the manufacturer's guide. The antisense oligonucleotides (ASO) targeting

133    human SNHG3 (ASO-SNHG3) and negative control ASO (ASO-NC) with no definite target

134    were adopted and purchased from RiboBio (Guangzhou，China). The ASO-SNHG3 sequence

135    was seen in **Supplementary Table 5**. For stable overexpression of SNHG3, the sequence of

136    this transcript was cloned into an adenovirus vector (Ad+). This bidirectional construct enables

137    a simultaneous and independent expression of the maker cassette for e-GFP-2A-Puro and of

138    SNHG3 (Ad-SNHG3) or a control sequence (Ad-GFP). All the in vitro experiments, unless

139   specified, were performed as at least three independent experiments with three replicates each

140   time.

141   **Inhibitors**

142   Cells were treated with 5-aza-2'-deoxycytidine, an inhibitor of DNA methyltransferases, for 24

143   hours at a concentration of 1 μM (Sigma-Aldrich, ON, Canada). For BMP pathway studies,

144   cells were treated with 100 ng/mL inhibitor LDN-193189 (Selleckchem, S2618, diluted in

145   DMSO) or 50 ng/mL human BMP2 (R&D, 355-BM-010), and control cells were treated with

146   equal volumes of DMSO (0.1% DMSO).

147   **Bisulfite sequencing PCR**

148   DNA was extracted hVICs with the DNeasy Blood and Tissue Kit (Qiagen, CA, USA) and

149   followed by bisulfate modification. The bisulfite sequencing analysis was performed with

150   EpiTect Bisulite Kit (Qiagen, CA, USA) following the provider's manual. The following

151   primers were used for PCR designed by MethPrimer (12):

152   Methylated BMP2 forward: 5'-TTTAGGGTTAGGAGAGCGAGG-3', reverse: 5'-

153   GACGATCTCGATACCAAACG-3'; Unmethylated BMP2 forward: 5'-

154   TTTAGGGTTAGGAGAGTGAGG-3', reverse: 5'-

155   ACAACAATCTCAATACCAAACAAAT-3'.

156   **Chromatin immunoprecipitation (ChIP) assay**

157   HVIC cells were transfected with Ad-SNHG3 or Ad-GFP. Cells were crosslinked with 1%

158   formaldehyde and further processed according to the supplier's protocol of the Pierce Agarose

159　CHIP Kit (Thermo Fisher Scientific, MA, USA) using H3K27me3 (5 μg, ab6002, abcam,

160　Cambridge, UK) and IgG antibody (5 μg, ab172730, abcam, Cambridge, UK) to investigate the

161　potential association between H3K27me3 and BMP2 promoter. The IgG antibody served as

162　control. The probe sequences used in our assay were listed below:

163　　Forward: 5'-CCTTGTTTGCGGTGCAATGA-3'

164　　Reverse: 5'-AGGCGAATTAGGCACTTGCT-3'

165　**SNHG3 pull-down**

166　Biotinylated RNA probes complementary to the back splice sequence of SNHG3 was designed

167　and synthesized by GenePharma(Suzhou, China). Pull down assay with the biotinylated

168　SNHG3 probe was performed with Pierce™ magnetic RNA-protein pull-down kit (Thermo

169　Scientific, USA) as previously described (13). Briefly, to generate probe-coated magnetic beads,

170　the Biotinylated-SNHG3 probe was resuspended in wash/binding buffer (0.5 mol/L NaCl, 20

171　mmol/L Tris-HCl, PH 7.5, and 1 mmol/L EDTA), followed by incubation with Dynabeads

172　MyOne Streptavidin C1 (Thermo Fisher, MA, USA) at 4℃ for 4 hours. Subsequently, hVICs

173　were lysed, sonicated, and then incubated with SNHG3 probe or oligo Probe at 4℃ overnight.

174　After treatment with the wash/binding buffer to wash and elute the RNA-binding protein

175　complexes, the protein complexes bound to the beads were isolated for further western blot

176　analysis according to standard procedures.

**RNA immunoprecipitation**

RNA immunoprecipitation (RIP) involved use of the Magna RIP RNA-Binding Protein Immunoprecipitation kit (Millipore, MA, USA). Briefly, RNA immunoprecipitation was performed in nuclear lysates of $10^7$ hVICs after SNHG3 knock-down (ASO treatment for 48 hours) or corresponding control group. HVICs were lysed in RIP lysis buffer before the supernatant was pre-cleared by protein G agarose beads. Then, the pre-cleared cell lysate was transferred to a tube containing antibody-immobilized protein G agarose beads. After overnight incubation at 4°C, the RNA-bound complex was washed, and stored for RNA isolation. The anti-EZH2 antibody (ab191250, abcam, Cambridge, UK) and control rabbit IgG (#PP64B, Merck Millipore) was used. The SNHG3 in EZH2 immunoprecipitated complex was measured by RT-qPCR.

**Immunofluorescence staining**

Immunofluorescence staining was applied for identifying hVICs isolation from human aortic valve with alpha smooth muscle actin (α-SMA) and Vimentin. Briefly, at the end of culture or treatment periods, hVICs were washed twice in PBS, fixed in 4% paraformaldehyde for 10 min and then permeabilized with 0.1% TritonX-100 in PBS for another 10 min. Next, the cells were incubated with primary antibodies against α-SMA (ab124964, 1:200, abcam) and Vimentin (ab8978, 1:200, abcam) followed by incubation with florescent conjugated secondary antibodies (1:150; abcam) and counterstaining with DAPI (Sigma). Images were taken with a

196 fluorescence microscope (Leica, SP8, Wetzlar, Germany) and merged using ImageJ software

197 (NIH).

198 **In silicon prediction of RNA-protein interaction**

199 The binding propensity between SNHG3 and EZH2 was predicted using software package

200 catRAPID (14) and RNA-Protein Interaction Prediction (RPISeq) (15). This algorithm

201 estimates the binding propensity of protein-RNA pairs considering secondary structures,

202 hydrogen bonds and van der Waals contributions. Amino acid-nucleotide interaction between

203 protein and RNA sequences are represented as interaction matrix.

204 **In silicon RNA secondary structure prediction**

205 RNA secondary structure was predicted by RNAfold WebServer (16)

206 (http://rna.tbi.univie.ac.at/cgi-bin/RNAfold.cgi) based on Minimum Free Energy (MFE) and

207 partition function.

208 **Animal experiments**

209 All animal studies were carried out in accordance with protocols approved by the Ethics

210 Committee of Fuwai Cardiovascular Hospital, Chinese Academy of Medical Sciences for the

211 Use and Care of Laboratory animals (NO. FW-2020-0022), and all the procedures complied

212 with US National Institutes of Health (NIH Publication No.85-23, revised 1996) on the

213 protection of animals used for scientific purposes. Adult ApoE$^{-/-}$ (C57BL/6 background) aged

214 eight weeks were purchased from Beijing Vital River Laboratory Animal Technology Co., Ltd.,

215 housed in a pathogen-free, temperature-controlled environment under a 12:12 hours light-dark

216    cycle. The mice were randomly allocated to 2 groups: mice fed normal diet (ND group, n=30);

217    mice fed 4% high cholesterol diet (HCD group, n=30). From the 12th week of the high-

218    cholesterol diet to the 24th week every 4 weeks, echocardiography was used to evaluate the

219    degree of aortic valve stenosis in the mice of the two groups and 6 mice in each group were

220    sacrificed at each time point in order to collect aortic valves to detect the expression level of

221    SNHG3 and osteogenic differentiation markers (ALP, RUNX2, osteopontin[OPN]) through

222    RT-qPCR. Another 6 mice in each group were sacrificed at 24th week of diet to collect aortic

223    valves making into paraffin slides for pathological staining.

224    Then ASO-SNHG3 (SNHG3 group, n=20) or ASO-NC (NC group, n=20) (5 nM/ injection) in

225    saline was injected into the lateral tail vein twice a week for 12 weeks from the 12th week of

226    high cholesterol diet. At the end of protocol, mice were euthanized by intravenous injection of

227    a lethal dose of pentobarbital sodium (100 mg/kg), and the aortic valves of 10 mice in each

228    group were used to extract RNA to detect expression levels of SNHG3 and osteogenic

229    differentiation markers, and the other 10 mice were used to make paraffin sections for

230    pathological staining.

231    **In situ hybridization of tissue sections**

232    The RNA scope probe target Mus-SNHG3 was designed and synthesized by Advanced Cell

233    Diagnostics company, and detection of SNHG3 expression was performed on an mice aortic

234    valve tissue sections using an RNAscope 2.5 High Definition (HD)-BROWN Assay kit

235    according to the manufacturer's instructions (Advanced Cell Diagnostics, Newark, CA, USA).

236    Briefly, tissues were fixed by 10% Neutral Buffered Formalin (NBF) followed by cell

237    pretreatment with pretreat NO.1 solution and pretreat NO.3 solution. Then, tissues were

238    hybridized with Mm-SNHG3-specific probe pairs, which were then hybridized to a cascade of

239    signal amplification molecules, culminating in binding of HRP-labeled probes. Finally, pictures

240    with DAB staining and hematoxylin counterstaining were taken. The images were acquired

241    with a Pannoramic MIDI Viewer (3D HISTECH Ltd., Budapest, Hungary). The signals were

242    visually scored based on the average number of dots per cell using the following criteria: 0 (no

243    staining or < 1 dot/10 cells), 1 (1–3 dots/cell), 2 (4–9 dots/cell. None or very few dot clusters),

244    3 (10–15 dots/cell and < 10% of the dots presented in clusters), 4 (> 15 dots/cell and > 10% of

245    the dots presented in clusters).

246    **Echocardiography**

247    Transthoracic echocardiography was performed under 2.5% isoflurane anesthesia, with an

248    18~38 MHZ phased-array probe (MS400) connected to a Vevo 2100 Imaging system

249    (VisualSonics, Toronto, Canada). Two-dimensional guided M-mode imaging was obtained in

250    the parasternal long- and short-views at the level of the papillary muscles. Left ventricular

251    internal diameters at end-diastole (LVIDd), Left ventricular internal diameters at end-systole

252    (LVIDs), Right ventricular internal diameters at end-diastole (RVIDd), Right ventricular

253    internal diameters at end-systole (RVIDs), ejection fraction (EF), fractional shortening (FS),

254    left ventricular stroke volume (SV), cardiac output (CO), and aortic valve area (AVA) were

255    calculated with the established standard equation. Peak velocity of E- and A- waves were

256    recorded by pulsed-wave Doppler in the apical 4-chamber view, and mitral annulus motion

257    velocity during early filing E' was measured using continuous-wave Doppler in the apical 5-

258    chamber view. All the measurements were made from 5 consecutive cardiac cycles and

259    averaged. The echocardiography analyses were evaluated by three individuals in a blinded

260    fashion.

261    **Hematoxylin and eosin, Von Kossa, Alizarin Red staining of aortic valves**

262    Aortic valves were rinsed in PBS, fixed in 4% paraformaldehyde, and embedded in paraffin.

263    Then the aortic valves were cut into 4 um slices and stained with hematoxylin and eosin (H&E),

264    Von Kossa and alizarin red staining as previously described (17,18). The thickness of the aortic

265    valve leaflets was measured as described previously (19). The leaflet sections were obtained

266    from each group, and leaflet thickness was determined using ImageJ 1.55 (NIH, Bethesda, MD,

267    USA) by three individuals in a blinded fashion. We analyzed mean aortic valve leaflet thickness

268    of 3 leaflets from each animal and used the mean thickness of ND group as a reference against

269    those of the HCD group, HCD + ASO-NC group and HCD + ASO-SNHG3 group.

270    **Statistical analysis**

271    Continuous data are presented as the mean value ± standard error of the mean (SEM) or mean

272    value ± standard deviation (SD) for normally distributed data. The normality of the distribution

273    of continuous data was confirmed by Shapiro-Wilk test and was visualized by a Q-Q plot. The

274    Levene test was used to confirm the homogeneity of variance of continuous data. For normally

275    distributed data, comparisons between the two groups were evaluated for significance using the

276  unpaired Student's t-test or Welch's t-test, whereas comparisons among three or more groups

277  were evaluated for significance using analysis of variance (ANOVA) followed by least

278  significance difference (LSD), Holm-Sidak, Dunett's test and Bonferroni multiple comparison

279  post hoc test using the SPSS software. The data that are not normality distributed were

280  compared using the Mann-Whitney U test (2 groups) or Kruskal-Wallis test (>2 groups). The

281  counts of category data were compared using chi-square analysis between two independent

282  groups. The association between the two continuous variables was evaluated using a two-tailed

283  Pearson's correlation analysis. Statistical significance was set at $p < 0.05$. Differential expression

284  analysis of lncRNAs in CAVD and non-mineralized control group using the limma R package

285  and the log2 fold change was computed as log2 (calcified aortic valve) minus log2 (non-

286  mineralized aortic valve).

287 **Supplementary Tables**

288 **Supplementary Table 1: Clinical characteristics of patients for lncRNA Sequencing**

| | Non-mineralized valves | Calcific valves | P |
|---|---|---|---|
| Sample, n | 12 | 10 | |
| Age, years | 48.5 ± 9.8 | 60.4 ± 4.8 | 0.002 |
| Male, n (%) | 10 (83.3) | 9 (90.0) | 0.65 |
| BMI, $Kg/m^2$ | 22.3 ± 2.8 | 24.6 ± 3.3 | 0.089 |
| Smoking, n (%) | 7 (58.3) | 8 (80) | 0.277 |
| Diabetes mellitus, n (%) | 3 (25) | 1 (10) | 0.724 |
| Hypertension, n (%) | 2 (16.7) | 6 (60) | 0.074 |
| Hyperlipidemia, n (%) | 4 (33.3) | 6 (60) | 0.412 |
| BAV, n (%) | 0 | 3 (30) | 0.078 |
| LVEF, % | 27.8 ± 8.03 | 62.3 ± 4.00 | ＜0.001 |
| Statins, n (%) | 5 (41.7) | 6 (60) | 0.392 |
| β-Blockers, n (%) | 4 (33.3) | 6 (60) | 0.412 |
| ACEi/ARB, n(%) | 5 (41.7) | 4 (40) | >0.99 |
| Transvalvular pressure gradient, mmHg | 15.26 ± 6.36 | 64.35 ± 16.86 | ＜0.001 |
| AVA, $cm^2$ | 3.28 ± 0.83 | 0.92 ± 0.31 | ＜0.001 |
| AS, n (%) | 0 | 10 | ＜0.001 |

289 Note: Values are means ± standard deviation or n (%).

290    Abbreviations: BMI, body mass index; LVEF, left ventricular ejection fraction; BAV, bicuspid

291    aortic valve; AS, aortic stenosis, AVA, aortic valve area.

292

293

294

295

296

297

298

299

300

301

302

303

304

305

306

307

308 **Supplementary Table 2: Clinical characteristics of patients for RT-qPCR analysis**

| | Non-mineralized valves | Calcific valves | P |
|---|---|---|---|
| Sample, n | 20 | 30 | |
| Age, years | 55.3 ± 8.2 | 58.4 ± 3.83 | 0.08 |
| Male, n (%) | 12 (60.0) | 18 (60.0) | >0.99 |
| BMI, Kg/m$^2$ | 22.6 ±2.9 | 23.5 ±2.7 | 0.27 |
| Smoking, n (%) | 10 (50.0) | 13 (43.3) | 0.64 |
| Diabetes mellitus, n (%) | 5 (25.0) | 6 (20.0) | 0.68 |
| Hypertension, n (%) | 8 (40.0) | 9 (30.0) | 0.47 |
| Hyperlipidemia, n (%) | 6 (30.0) | 8 (26.7) | 0.80 |
| BAV, n (%) | 0 | 3 (10) | 0.16 |
| LVEF, (%) | 30.1 ± 7.4 | 64.5 ± 8.3 | <0.001 |
| Statins, n(%) | 6 (30) | 8 (26.7) | 0.80 |
| β-Blockers, n (%) | 12 (60) | 16 (53.3) | 0.64 |
| ACEi/ARB, n(%) | 11 (55.5) | 18 (60) | 0.73 |
| Transvalvular pressure gradient (mmHg) | 13.36 ± 3.82 | 73.24 ± 26.31 | <0.001 |
| AVA, cm$^2$ | 3.69 ± 0.46 | 0.68 ± 0.21 | <0.001 |
| AS, n (%) | 0 | 30 | <0.001 |

309 Note: Values are means ± standard deviation or n (%).

310    Abbreviations: BMI, body mass index; LVEF, left ventricular ejection fraction; BAV, bicuspid

311    aortic valve; AS, aortic stenosis, AVA, aortic valve area.

312

313

314

315

316

317

318

319

320

321

322

323

324

325

326

327

328

329 **Supplementary Table 3: Clinical characteristics of patients for cell cultures**

| Parameters | Non-mineralized valve |
|---|---|
| Sample, n | 10 |
| Age, y | 47.1 ± 13.2 |
| Male, n (%) | 6 (60) |
| BMI, kg/m$^2$ | 23.1 ± 3.0 |
| Smoking, n (%) | 1(10) |
| Diabetes mellitus, n (%) | 5 (50) |
| Hypertension, n (%) | 3 (30) |
| Hyperlipidemia, n (%) | 2 (20) |
| BAV, n (%) | 0 |
| LVEF (%) | 29.1 ± 6.0 |
| Statins, n(%) | 4 (40) |
| β-Blockers, n (%) | 4 (40) |
| ACEi/ARB, n(%) | 5 (50) |
| Transvalvular pressure grandient, mmHg | 12.38 ± 3.82 |
| AVA, cm$^2$ | 3.37 ± 0.51 |
| AS, n (%) | 0 |

330 Note: Values are means ± standard deviation or n (%).

331    Abbreviations: BMI, body mass index; LVEF, left ventricular ejection fraction; BAV, bicuspid

332    aortic valve; AS, aortic stenosis; AVA, aortic valve area.

333

334

335

336

337

338

339

340

341

342

343

344

345

346

347

348

349

**Supplementary Table 4. Differentially expressed lncRNAs between calcified aortic valves**

**and non-mineralized control.**

| Gene | Log2foldchange | P. Value | Adj. P. Value |
|---|---|---|---|
| H19 | 3.095080069 | 1.27E-05 | 0.002893561 |
| SFTA1P | 2.078357747 | 8.24E-05 | 0.008404232 |
| SNHG3 | 1.890750966 | 1.84E-14 | 8.09E-10 |
| AC004988.1 | 1.801660853 | 1.23E-06 | 0.000834623 |
| LINC01060 | 1.693807801 | 0.005913671 | 0.104436661 |
| AP001189.4 | 1.661672703 | 0.000300255 | 0.018265794 |
| LINC00702 | 1.641611262 | 0.002672971 | 0.066993535 |
| LINC01592 | 1.636321881 | 0.000904209 | 0.035185738 |
| LINC01450 | 1.525521068 | 0.000212985 | 0.014449838 |
| UNC5B-AS1 | 1.453359057 | 3.04E-07 | 0.000343734 |
| LINC01614 | 1.44707174 | 0.002516282 | 0.064887073 |
| AC012462.2 | 1.435872021 | 6.83E-05 | 0.007669113 |
| RGS5 | 1.364045163 | 0.001631298 | 0.050491125 |
| FAM225A | 1.323248632 | 0.000183963 | 0.013364686 |
| LZTS1-AS1 | 1.310162878 | 3.46E-05 | 0.005108973 |
| AC005943.2 | 1.251417445 | 0.041866232 | 0.288253291 |
| AC007906.1 | 1.249434364 | 0.001488356 | 0.04802429 |
| LINC00545 | 1.22294784 | 2.86E-05 | 0.004640681 |
| TYMSOS | 1.212602671 | 0.000834824 | 0.033456756 |
| AC017002.2 | 1.202186143 | 5.67E-05 | 0.006876721 |
| AC067945.3 | 1.162936697 | 0.010007272 | 0.140642553 |
| FNDC1-IT1 | 1.154301758 | 0.004839106 | 0.094599896 |
| ZNF385D-AS2 | 1.14573453 | 0.013991332 | 0.165520879 |
| LINC01142 | 1.129646762 | 0.00413888 | 0.086682271 |
| FAM155A-IT1 | 1.110151521 | 0.001806903 | 0.053831945 |
| LINC01117 | 1.108203957 | 0.002192267 | 0.059909905 |
| AC133644.2 | 1.102213569 | 1.52E-05 | 0.003170867 |
| LRP1-AS | 1.081972489 | 2.94E-05 | 0.004707311 |
| AC108463.2 | 1.071664879 | 0.020619419 | 0.202729052 |
| AC002401.1 | 1.027838518 | 0.004595577 | 0.092003446 |
| LINC01561 | 1.020160488 | 0.009600917 | 0.138461952 |
| HOTAIRM1 | 1.01893228 | 0.002534751 | 0.065103844 |
| LINC01259 | 1.007982903 | 0.014327209 | 0.167724033 |
| C11orf40 | -1.000468083 | 0.005850269 | 0.103815173 |
| FLJ31356 | -1.007428487 | 0.002186818 | 0.05986091 |

| | | | |
|---|---|---|---|
| C15orf56 | -1.009153588 | 0.006862973 | 0.114540646 |
| AL022397.1 | -1.018028489 | 0.002052048 | 0.057899034 |
| VIPR1-AS1 | -1.021291504 | 0.003788128 | 0.082108419 |
| AC091493.1 | -1.032572762 | 0.000897582 | 0.035016029 |
| AC103563.9 | -1.04375828 | 0.003703039 | 0.081102271 |
| LINC00689 | -1.047114588 | 4.51E-05 | 0.006038358 |
| LINC01153 | -1.047151935 | 0.009499969 | 0.137614697 |
| RAMP2-AS1 | -1.049634006 | 4.13E-05 | 0.00562999 |
| TRHDE-AS1 | -1.061285929 | 1.02E-05 | 0.002686769 |
| NRG1-IT1 | -1.088310277 | 0.010995953 | 0.147293427 |
| LINC01392 | -1.093870003 | 0.00070731 | 0.030333763 |
| AC004870.4 | -1.112944809 | 0.012477281 | 0.156077636 |
| LINC01625 | -1.150741749 | 0.000188961 | 0.013466998 |
| AC079117.1 | -1.158275136 | 0.013582956 | 0.163589745 |
| ELOVL2-AS1 | -1.160981239 | 8.84E-07 | 0.000670958 |
| LINC01030 | -1.183685274 | 0.003860819 | 0.08294923 |
| LINC01168 | -1.200877893 | 0.010071442 | 0.141172573 |
| AC019055.1 | -1.206775032 | 0.000559033 | 0.026187474 |
| AC008691.1 | -1.217914822 | 0.002374935 | 0.062786107 |
| LINC01539 | -1.226622798 | 0.017395325 | 0.18537617 |
| LINC00334 | -1.237072624 | 0.012247765 | 0.154976299 |
| ZNF341-AS1 | -1.283575242 | 0.007217838 | 0.11774165 |
| GACAT3 | -1.286640812 | 0.000406491 | 0.022130405 |
| ARHGAP26-AS1 | -1.324184668 | 0.001471382 | 0.047791703 |
| LINC01049 | -1.332279028 | 0.004640936 | 0.092449292 |
| PLCH1-AS1 | -1.357912806 | 5.42E-05 | 0.006693954 |
| PLCH1-AS2 | -1.388409005 | 0.005032948 | 0.09629504 |
| CACNA2D3-AS1 | -1.407034465 | 0.000402347 | 0.021990376 |
| AC011625.1 | -1.499429051 | 1.89E-05 | 0.003590072 |
| MAPT-IT1 | -1.53794834 | 8.82E-05 | 0.008655374 |
| DIO3OS | -1.539817216 | 7.43E-05 | 0.008113913 |
| UNQ6494 | -1.576356643 | 0.000101357 | 0.009478095 |
| TUSC7 | -1.665780284 | 0.000159296 | 0.012259636 |
| ALDH1L1-AS2 | -1.695083967 | 3.96E-05 | 0.00556104 |
| LINC00844 | -1.713622132 | 0.000556809 | 0.026145087 |
| CNTFR-AS1 | -1.898973991 | 0.000357223 | 0.020145341 |
| WNT5A-AS1 | -2.015737953 | 1.19E-05 | 0.002785613 |

352

**Supplementary Table 5: Primes and probes for RT-qPCR and antisense oligonucleotides for mus- and homo- SNHG3.**

| Primers for qPCR | Primer sequence (5′ to 3′) |
| --- | --- |
| Homo-SNHG3 forward | TTCAAGCGATTCTCGTGCC |
| Homo-SNHG3 reverse | AAGATTGTCAAACCCTCCCTGT |
| Homo-SFTA1P forward | CAGCATTCCAGGTGGGCTTT |
| Homo-SFTA1P reverse | CCTTGTTTGGCTTACTCGTGC |
| Homo-AC004988.1 forward | TAATGGCATGCAGAGCGGAG |
| Homo-AC004988.1 reverse | TTTTCACGGATTCCACCCCA |
| Homo-LINC01060 forward | TCCCGCTCTAATGATCACGC |
| Homo-LINC01060 reverse | TGTTACTCTCTGAGTCCTGTGA |
| Homo-AP001189.4 forward | AGGAACCCTGCCACATCATG |
| Homo-AP001189.4 reverse | TCACAAACCTATGGGGCCAC |
| Homo-LINC00702 forward | ATTCACATCCGGGGCCAATT |
| Homo-LINC00702 reverse | AGGAACTGCTCAATGCTGCT |
| Homo-LINC01592 forward | GTGCATGAGACTGAGACAGGT |
| Homo-LINC01592 reverse | AGGCAGTTGAAATTTTGAGCAA |
| Homo-LINC01450 forward | GGAAGACCCGCTGATGAGTC |
| Homo-LINC01450 reverse | AAAAGACTCACCCTGTGCCC |
| Homo-UNC5B-AS1 forward | CAAGCCTGCCTTCTTGGAGA |

| | |
|---|---|
| **Homo-UNC5B-AS1 reverse** | GGCAGGATCTTTTTGGGGGA |
| **Homo-BMP2 forward** | ACCCGCTGTCTTCTAGCGT |
| **Homo-BMP2 reverse** | TTTCAGGCCGAACATGCTGAG |
| **Homo-ALPL forward** | TTGTGCCAGAGAAAGAGAGAGA |
| **Homo-ALPL reverse** | GTTTCAGGGCATTTTTCAAGGT |
| **Homo-SPP1 forward** | CTCCATTGACTCGAACGACTC |
| **Homo-SPP1 reverse** | CAGGTCTGCGAAACTTCTTAGAT |
| **Homo-BGLAP forward** | CACTCCTCGCCCTATTGGC |
| **Homo-BGLAP reverse** | CCCTCCTGCTTGGACACAAAG |
| **Homo-GAPDH forward** | TGATGACATCAAGAAGGTGG |
| **Homo-GAPDH reverse** | TTGTCATACCAGGAAATGAGC |
| **Homo-U6 forward** | CGCTTCGGCAGCACATATAC |
| **Homo-U6 reverse** | TTCACGAATTTGCGTGTCATC |
| **Homo-H19 forward** | TGCTGCACTTTACAACCACTG |
| **Homo-H19 reverse** | ATGGTGTCTTTGATGTTGGGC |
| **Mus-SNHG3 forward** | TCCGGGCGTTACTTAAGGTATA |
| **Mus-SNHG3 reverse** | GCCGAGGCTGTAACAGACAA |
| **Mus-ALPL forward** | GTGACTACCACTCGGGTGAAC |
| **Mus-ALPL reverse** | CTCTGGTGGCATCTCGTTATC |
| **Mus-BMP2 forward** | GGGACCCGCTGTCTTCTAGT |

25

| | |
|---|---|
| **Mus-BMP2 reverse** | TCAACTCAAATTCGCTGAGGAC |
| **Mus-SPP1 forward** | AGCAAGAAACTCTTCCAAGCAA |
| **Mus-SPP1 reverse** | GTGAGATTCGTCAGATTCATCCG |
| **Mus-BGLAP forward** | GAACAGACAAGTCCCACACAGC |
| **Mus-BGLAP reverse** | TCAGCAGAGTGAGCAGAAAGAT |
| **Mus-RUNX2 forward** | GACTGTGGTTACCGTCATGGC |
| **Mus-RUNX2 reverse** | ACTTGGTTTTTCATAACAGCGGA |
| **Mus-GAPDH forward** | CCCTTAAGAGGGATGCTGCC |
| **Mus-GAPDH reverse** | ACTGTGCCGTTGAATTTGCC |
| **ASO for SNHG3 mice** | TGAGGTCCCAACAGGTTTCC |
| **ASO for SNHG3 human** | CCAGCCCTCATACCTCTTTT |
| **ASO for H19 human** | CCACGGAGTCGGCACACTAT |
| **ASO for SFTA1P human** | GGAATCTGCATTTCTTTCAG |

355

356

357

358

359

26

**Supplementary Table 6: Comparison of echocardiographic in ApoE$^{-/-}$ mice of different groups at 24th of high-cholesterol diets.**

| Parameter | ND (N=6) | HCD (N=6) | HCD+ASO-NC (N=10) | HCD+ASO-SNHG3 (N=10) |
|---|---|---|---|---|
| Body weight, g | 29.21 ± 0.58 | 40.42 ± 2.37 | 40.35 ± 1.78 | 36.97 ± 1.50 |
| Heart rate, bmp | 533.14 ± 12.57 | 539.77 ± 16.54 | 536.34 ± 10.59 | 535.19 ± 19.31 |
| LVEDd, mm | 3.27 ± 0.32 | 3.21 ± 0.13 | 3.22 ± 0.08 | 3.13 ± 0.09 |
| FS, % | 46.20±1.62 | 45.82 ± 1.36 | 46.53 ± 1.83 | 45.93 ± 1.63 |
| LVEF, % | 70.32 ± 3.34 | 69.86 ± 4.35 | 72.26 ± 4.68 | 71.23 ± 3.76 |
| SV, ml | 0.05 ± 0.01 | 0.05 ± 0.01 | 0.05 ± 0.02 | 0.05 ± 0.01 |
| CO, ml/min | 28.48 ± 2.13 | 28.37 ± 1.03 | 28.13 ± 1.76 | 28.03 ± 1.88 |
| Aortic valve velocity, mm/s | 1094 ± 30.37 | 2196 ± 43.87* | 2287 ± 27.76 | 1411 ± 23.58** |
| AVA, mm$^2$ | 1.45 ± 0.05 | 0.87 ± 0.06* | 0.89 ± 0.01 | 1.12 ± 0.01** |

Note: Data are presented mean ± standard error of the mean.

Abbreviations: ApoE$^{-/-}$, apolipoprotein E-deficient; ND, normal diet; HCD, high-cholesterol diet; ASO, antisense oligonucleotide; NC, negative control; SNHG3, Small Nucleolar RNA Host Gene 3; LVEDd, left ventricular end-diastolic diameter; FS, functional shortening; LVEF, left ventricular ejection fraction, SV, stroke volume; CO: cardiac output; AVA, aortic valve area.* $p < 0.05$ vs. ND group.**$p < 0.05$ vs. HCD+ASO-NC group. Unpaired two-tailed Student's t-test.

370 **Supplementary Table 7: Metabolic parameters in different groups of ApoE$^{-/-}$ mice at 24th**

371 **of high-cholesterol diets.**

| Parameters | ND (n=6) | HCD (n=6) | HCD+ASO-NC (n=10) | HCD+ASO-SNHG3 (n=10) |
|---|---|---|---|---|
| Glucose, mmol/L | 10.66 ± 1.95 | 10.16 ± 1.82 | 10.58 ± 2.16 | 10.28 ± 2.23 |
| TC, mmol/L | 13.38 ± 1.65 | 28.15 ± 2.78 | 28.63 ± 3.12 | 29.12 ± 3.22 |
| LDL, mmol/L | 8.15 ± 1.36 | 25.82 ± 3.45 | 26.55 ± 3.32 | 26.39 ± 3.55 |
| TG, mmol/L | 1.23 ± 0.25 | 2.18 ± 0.32 | 2.08 ± 0.57 | 2.16 ± 0.48 |

372 Note: Data are presented mean ± standard error of the mean.

373 Abbreviations: ApoE$^{-/-}$, apolipoprotein E-deficient; ND, normal diet; HCD, high-cholesterol

374 diet; ASO, antisense oligonucleotide; NC, negative control; SNHG3, Small Nucleolar RNA

375 Host Gene 3.

376

377

378

379

380

381

382 **Supplementary Figures**

383 **Supplementary Figure 1**

384 **Human calcific aortic valves were confirmed by both Alizarin red and Von Kossa staining.**

385 **Scale bar: 100 μm.**
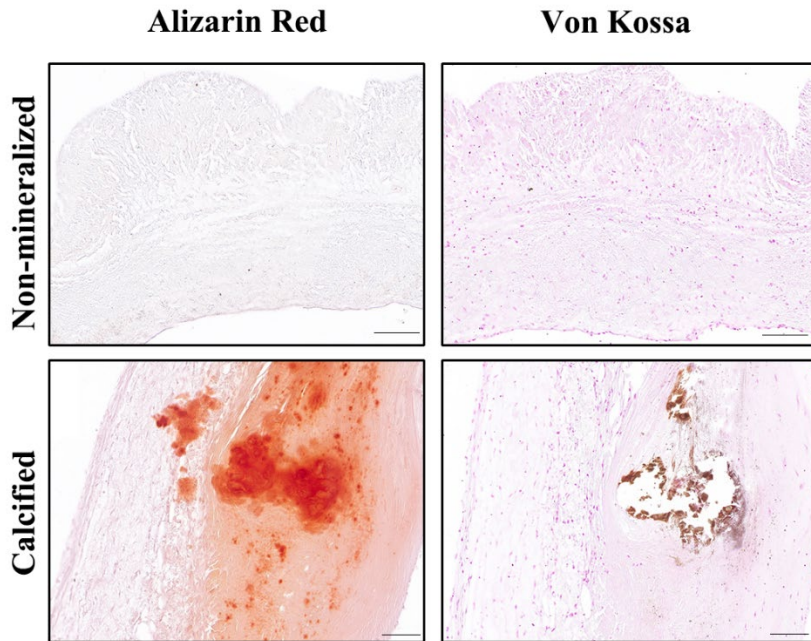


386
387

388

389

390

391    **Supplementary Figure 2**

392    **Immunofluorescence staining showed that hVICs were positive for both alpha smooth**

393    **muscle actin (α-SMA; green) and vimentin (red).** DAPI was used for nuclear counterstaining

394    (blue). Scale bar: 25 μm.



| DAPI | α-SMA | Vimentin | Merge |
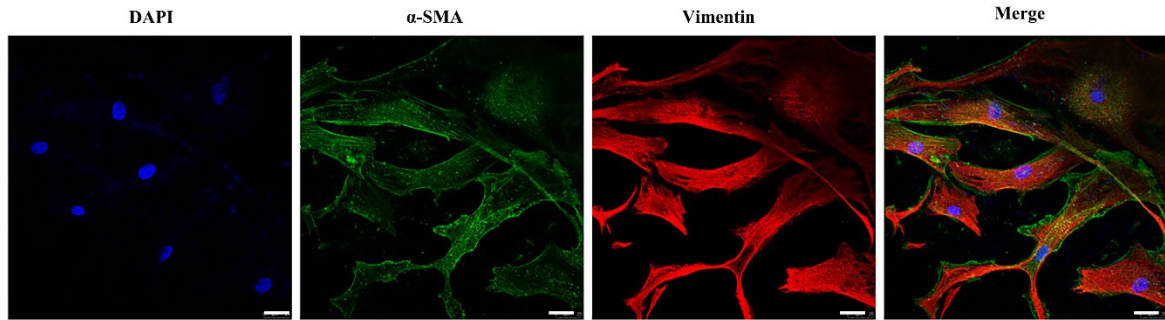
395

396

397

398

399

400

401

402

403

404

405

406

407

408    **Supplementary Figure 3**

409    **Candidate gene selection post differential expression analysis.** (A-J) RT-qPCR validation

410    of top 10 upregulated lncRNAs in calcific (N=30) and non-mineralized (N=20) aortic valve

411    tissues. Unpaired two-tailed Student's t-test. Three osteogenic differentiation markers (alkaline

412    phosphatase [ALP], RUNX2, and osteopontin [OPN] ) mRNA levels in hVICs transfected with

413    antisense oligonucleotide (ASO) targeting (K) H19, (L) SFTA1P, (M) SNHG3 (N=6/group).

414    Unpaired two-tailed Student's t-test. Corrected for multiple comparisons using the Holm-Sidak

415    method (3 tests) for K, L and M.*** p<0.001. Values are the mean ± SEM.
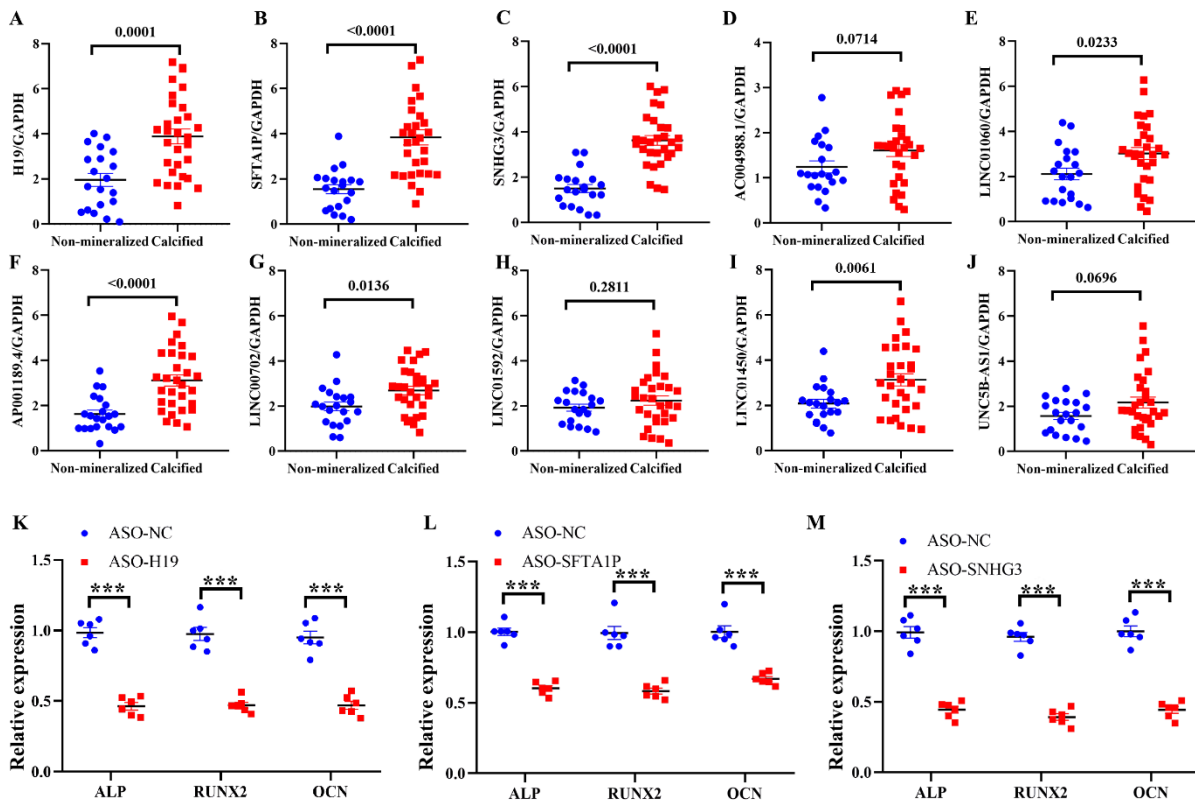


416

417

418

419 **Supplementary Figure 4**

420 **Representative echocardiographic images of transvalvular peak jet velocity in ApoE-/-**

421 **mice from 12th week to 24 week of high-cholesterol diet (HCD) and Normal diet (ND).**

422 The transvalvular peak jet velocity is significant higher in HCD group than that in ND group

423 and the aortic valve area (AVA) is more smaller in HCD group than that in ND group, which

424 show the mice have severe aortic valve calcification arising from HCD diet. N=6/group. Values

425 are mean ± SEM. *** P<0.001 between ND and HCD group at indicated timepoint with two-

426 way ANOVA corrected for multiple comparisons using the least significant difference (LSD)

427 test.
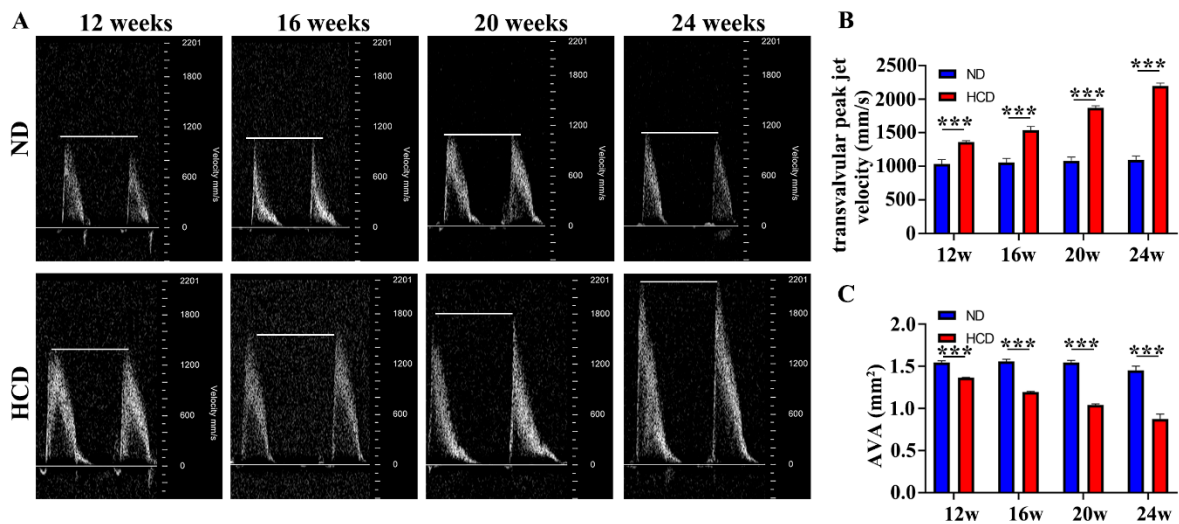
434    **Supplementary Figure 5**

435    **Gene set enrichment analysis (GSEA) of osteoblast differentiation**. GSEA revealed the

436    calcium signaling pathway (A), MAPK signaling pathway(B), gene set of aortic valve stenosis

437    (C) and increased bone mineral density (D) significantly upregulated in condition of SNHG3-

438    overexpressed hVICs with adenovirus (ADV) compared with Ad-GFP.
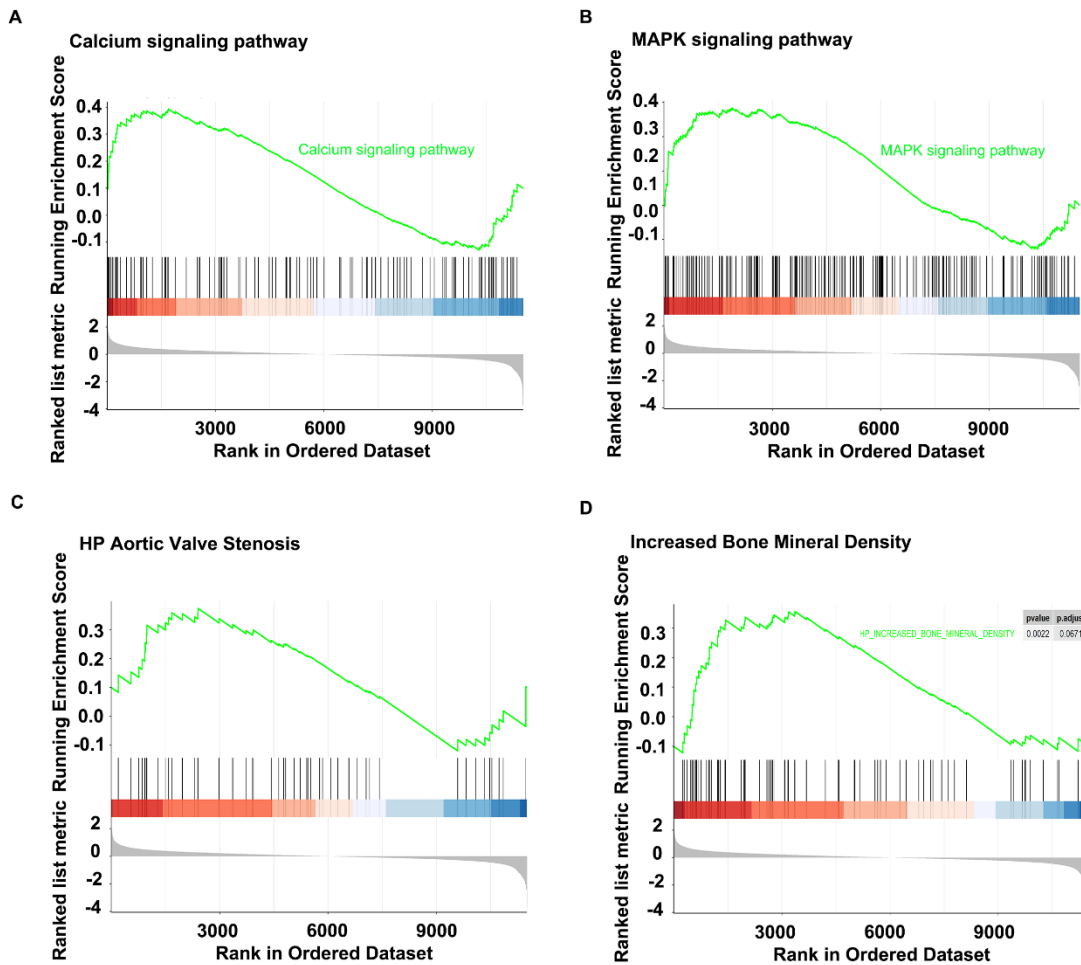


439

440

441    **Supplementary Figure 6**

442    **Kyoto Encyclopedia of Genes and Genomes (KEGG) enrichment analysis of osteoblast**
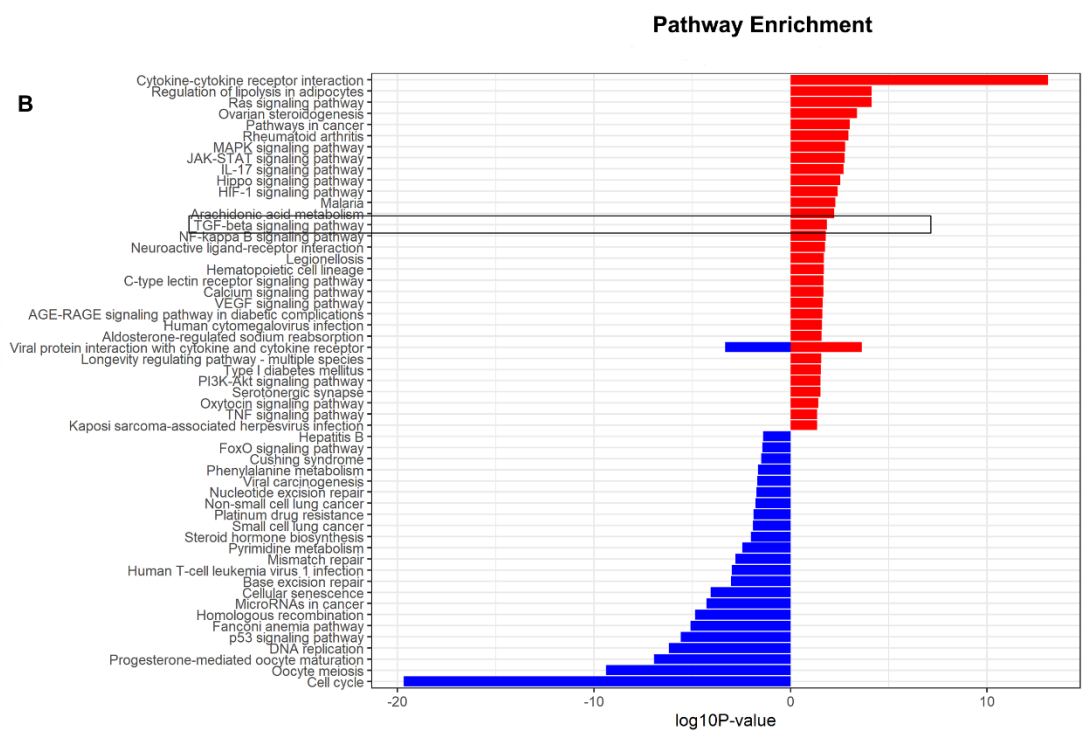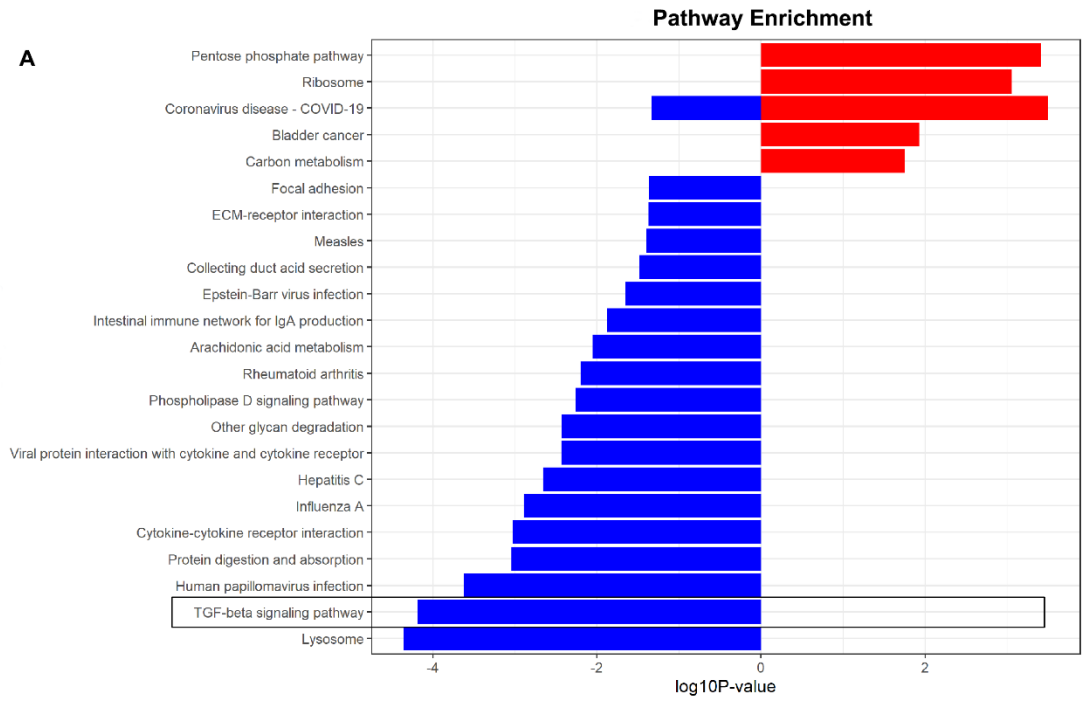
443    **differentiation.** A) KEGG enrichment analysis of TGF-β signaling pathway was significantly

444    downregulated in case of SNHG3 knockdown with antisense oligonucleotide (ASO). B) KEGG

445    of TGF-β signaling pathway was significantly upregulated in condition of SNHG3

446    overexpression with adenovirus (ADV).

447

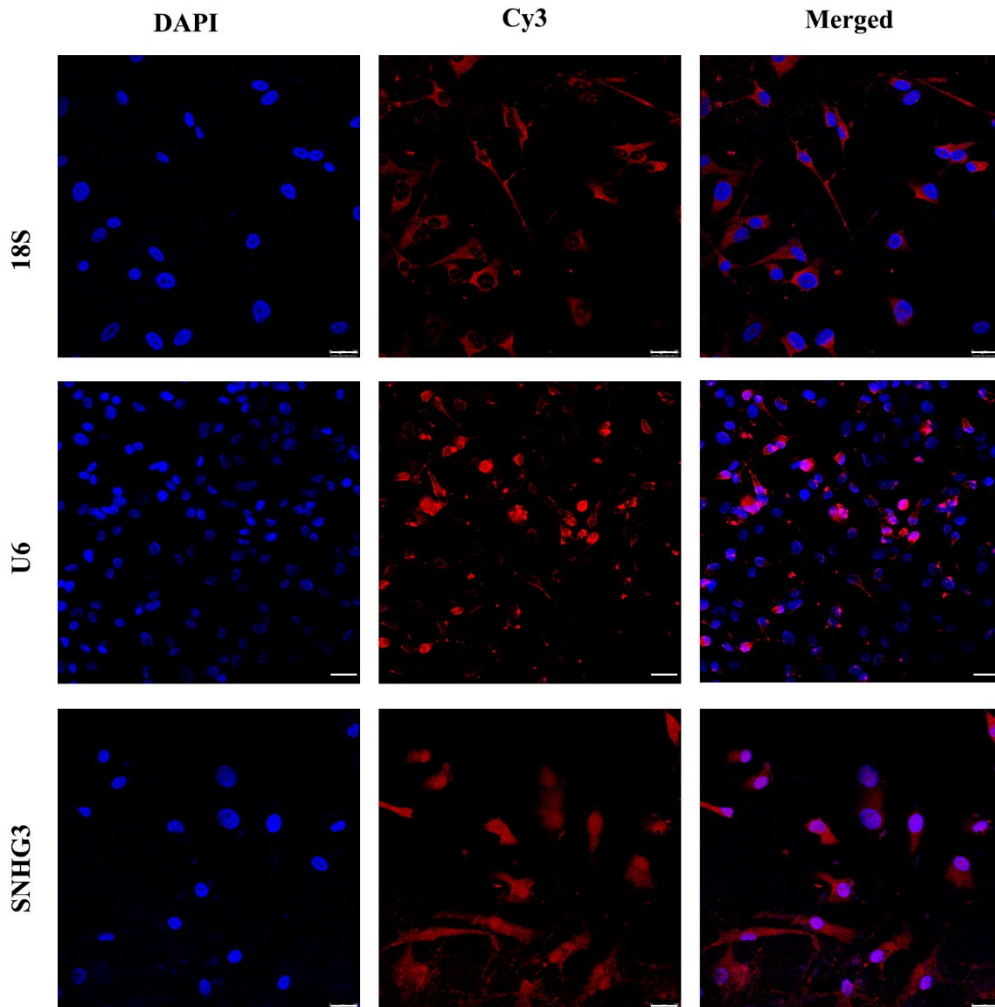**Pathway Enrichment**



**Pathway Enrichment**

448

449　**Supplementary Figure 7**

450　**Endogenous SNHG3 (red) in hVICs detected by RNA-FISH.** Probes for 18S (red) and U6

451　(red) serve as cytoplasmic and nuclear controls, respectively. Scale bar, 25 μm.



452

453

454

455

456 **Supplementary Figure 8**

457 **Promoting calcification culture of hVICs does not change subcellular abundance of**

458 **SNHG3 in vitro.** Cytoplasmatic, nuclear RNA abundance of SNHG3 compared to nuclear

459 marker U6 and cytoplastic marker GAPDH in subcellular fractions of hVICs after osteogenic

460 stimulation with osteogenic induction medium for 72 hours (n=3). Data are means ± SD.

461
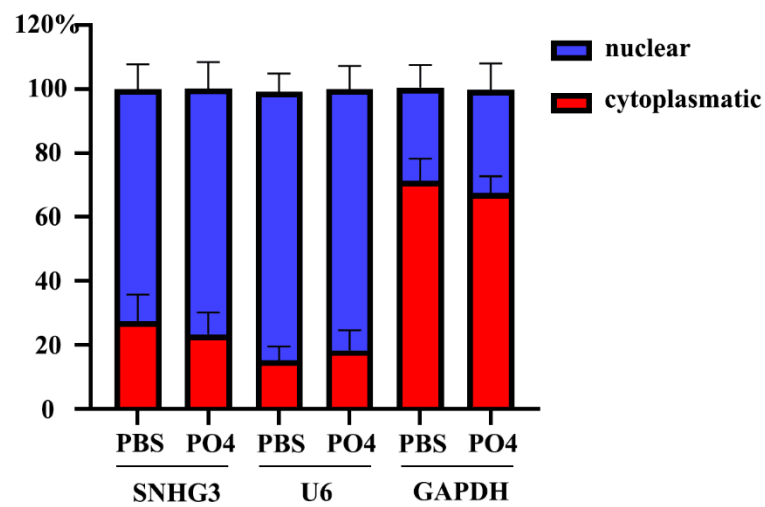


462
463
464
465
466
467
468

469     **Supplementary Figure 9**

470     **EZH2 interacts directly with SNHG3 based on Sequence and Structure.** A) Sequence-

471     based prediction of SNHG3-EZH2 interaction, with random forest, RF classifier score 0.85 and

472     support vehicle machine, SVM classifier score of 0.96. *Interaction probabilities generated by

473     RPISeq range from 0 to 1. In performance evaluation experiments, predictions with

474     probabilities >0.5 were considered positive, i.e., indicating that the corresponding RNA and

475     protein are likely to interact. B) CatRAPID fragment tool reveals that EZH2 region (amino-acid

476     residues 326-377) and SNHG3 region (1932-2025) have the highest interaction propensity,

477     discriminative power, Normalized Score. C) Predicted RNA structure of the motif identified in

478     SNHG3 region (1932-2025) responsible for its interaction with EZH2. D) EZH2 region (amino-

479     acid residues 326-377) interacted with SNHG3 included a Thr-345, a conservative CDK

480     phosphorylation site, which can be phosphorylated by AKT1 and promote maintenance of

481     H3K27m3 levels at EZH2-target loci, thus leading to epigenetic gene silencing.

**A**

RNA-Protein Interaction Prediction
(RPISeq)

## Inpt Sequences

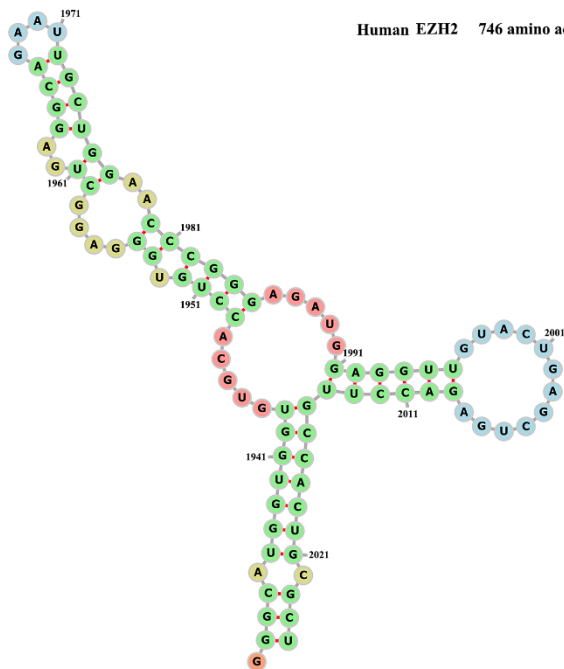Protein: (EZH2): NCB1Ref. Seq.

NP_001190176

RNA: (SNHG3): NCBI Ref. Seq.

NR_036473.1

| Interaction Probability (EZH2:SNHG3) | |
|---|---|
| RF clssififier Prediction | *0.85 |
| SVM classifier Prediction | *0.96 |

**B**

| | EZH2 region | SNHG3 region | Interaction Propensity | Discriminative Power | Normalized Score |
|---|---|---|---|---|---|
| 1 | 326-377 | 1932-2025 | 26.05 | 67 | 4.21 |
| 2 | 326-377 | 1933-2026 | 24.15 | 63 | 3.90 |
| 3 | 226-277 | 1932-2025 | 21.60 | 56 | 3.49 |
| 4 | 496-547 | 1932-2025 | 21.33 | 56 | 3.45 |
| 5 | 321-372 | 1932-2025 | 20.12 | 54 | 3.25 |
| 6 | 46-97 | 1932-2025 | 19.84 | 52 | 3.21 |
| 7 | 496-547 | 1933-2026 | 19.53 | 52 | 3.16 |
| 8 | 196-247 | 1932-2025 | 19.18 | 52 | 3.10 |
| 9 | 226-277 | 1933-2026 | 18.73 | 50 | 3.03 |
| 10 | 126-177 | 1932-2025 | 18.61 | 50 | 3.01 |

**C**



**D**

Human EZH2    746 amino acid

| EID | Domain I | Domain II | | CXC | SET |

|  | | | * | |
| Human | 341 | ERIKTPPKRP |
| Mouse | 341 | ERIKTPPKRP |
| Rat | 341 | ERIKTPPKRP |
| Pig | 357 | ERIKTPPKRP |
| Bovin | 352 | ERIKTPPKRP |
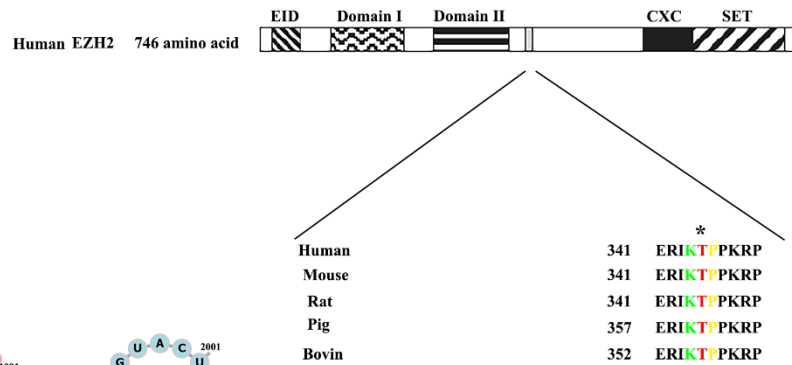
482

483

484

485

486

487

39

**Reference**

1. Mahmut A, Boulanger MC, Bouchareb R, Hadji F, Mathieu P. Adenosine derived from ecto-nucleotidases in calcific aortic valve disease promotes mineralization through A2a adenosine receptor. Cardiovasc Res 2015;106:109-20.

2. Hadji F, Boulanger MC, Guay SP et al. Altered DNA Methylation of Long Noncoding RNA H19 in Calcific Aortic Valve Disease Promotes Mineralization by Silencing NOTCH1. Circulation 2016;134:1848-1862.

3. Kim D, Pertea G, Trapnell C, Pimentel H, Kelley R, Salzberg SL. TopHat2: accurate alignment of transcriptomes in the presence of insertions, deletions and gene fusions. Genome Biol 2013;14:R36.

4. Pertea M, Kim D, Pertea GM, Leek JT, Salzberg SL. Transcript-level expression analysis of RNA-seq experiments with HISAT, StringTie and Ballgown. Nat Protoc 2016;11:1650-67.

5. Sun L, Luo H, Bu D et al. Utilizing sequence intrinsic composition to classify protein-coding and long non-coding transcripts. Nucleic Acids Res 2013;41:e166.

6. Kong L, Zhang Y, Ye ZQ et al. CPC: assess the protein-coding potential of transcripts using sequence features and support vector machine. Nucleic Acids Res 2007;35:W345-9.

7. Finn RD, Bateman A, Clements J et al. Pfam: the protein families database. Nucleic Acids Res 2014;42:D222-30.

508   8.    Lin MF, Jungreis I, Kellis M. PhyloCSF: a comparative genomics method to distinguish

509          protein coding and non-coding regions. Bioinformatics 2011;27:i275-82.

510   9.    Ritchie ME, Phipson B, Wu D et al. limma powers differential expression analyses for

511          RNA-sequencing and microarray studies. Nucleic Acids Res 2015;43:e47.

512   10.   Subramanian A, Tamayo P, Mootha VK et al. Gene set enrichment analysis: a

513          knowledge-based approach for interpreting genome-wide expression profiles. Proc Natl

514          Acad Sci U S A 2005;102:15545-50.

515   11.   Liberzon A, Birger C, Thorvaldsdottir H, Ghandi M, Mesirov JP, Tamayo P. The

516          Molecular Signatures Database (MSigDB) hallmark gene set collection. Cell Syst

517          2015;1:417-425.

518   12.   Li LC, Dahiya R. MethPrimer: designing primers for methylation PCRs. Bioinformatics

519          2002;18:1427-31.

520   13.   Liu H, Xu Y, Yao B, Sui T, Lai L, Li Z. A novel N6-methyladenosine (m6A)-dependent

521          fate decision for the lncRNA THOR. Cell Death Dis 2020;11:613.

522   14.   Agostini F, Zanzoni A, Klus P, Marchese D, Cirillo D, Tartaglia GG. catRAPID omics:

523          a web server for large-scale prediction of protein-RNA interactions. Bioinformatics

524          2013;29:2928-30.

525   15.   Muppirala UK, Honavar VG, Dobbs D. Predicting RNA-protein interactions using only

526          sequence information. BMC bioinformatics 2011;12:489.

527   16.   Will S, Jabbari H. Sparse RNA folding revisited: space-efficient minimum free energy

528         structure prediction. Algorithms Mol Biol 2016;11:7.

529   17.    Wang Y, Han D, Zhou T et al. Melatonin ameliorates aortic valve calcification via the

530         regulation of circular RNA CircRIC3/miR-204-5p/DPP4 signaling in valvular

531         interstitial cells. J Pineal Res 2020;69.

532   18.    Yu C, Li L, Xie F et al. LncRNA TUG1 sponges miR-204-5p to promote osteoblast

533         differentiation through upregulating Runx2 in aortic valve calcification. Cardiovasc Res

534         2018;114:168-179.

535   19.    Isoda K, Matsuki T, Kondo H, Iwakura Y, Ohsuzu F. Deficiency of interleukin-1

536         receptor antagonist induces aortic valve disease in BALB/c mice. Arterioscler Thromb

537         Vasc Biol 2010;30:708-15.